RF Field Analysis for High Field Magnetic Resonance Imaging Systems

#Hyoungsuk Yoo [1], J. Thomas Vaughan [2], and Anand Gopinath [3]
[1] School of Electrical Engineering, Department of Biomedical Engineering, University of Ulsan
Ulsan 680-479, South Korea, hsyoo@ulsan.ac.kr
[2] Center for Magnetic Resonance Research, Department of Radiology, University of Minnesota
Minneapolis, MN 55455 USA, tommy@cmrr.umn.edu
[3] Department of Electrical and Computer Engineering, University of Minnesota
Minneapolis, MN 55455 USA, gopinath@umn.edu

Abstract

The combined field integral equation method is used to calculate the RF B_1 field produced by a transmission line resonator element for high field magnetic resonance systems. The proposed method provides faster electromagnetic field results than the finite difference time domain approach. A field localization method is also discussed.

Keywords : Magnetic resonance imaging (MRI), integral equation, method of moments, localization, transmission line element, RF B_1 field

1. Introduction

Magnetic resonance imaging (MRI) is an important tool in clinical diagnosis and high field MRIs (4 T and above) provide better signal to noise ratios (SNR) and higher resolution in the images [1]–[3]. However, as the Larmor frequency is proportional to the static field (B_0) field, at high fields, efficient radio frequency (RF) resonator design, close to the human subjects, is challenging due to the short wavelength in the human body and also due to inter-element coupling. A lumped elements resonator is widely used in the low B_0 field (1.5 T and 3.0 T) clinical MRI systems. To simulate the RF magnetic field (B_1) in phantoms and the human body, the finite-diffrence time domain (FDTD) method and the finite-element method (FEM) are widely used and these methods require the entire computational domain to be discretized. However, the computational costs become severe in RF multi-channel coils. An alternative is the solution of the combined field integral equation (CFIE) to obtain the surface current distribution on phantoms and the human head and body [4].

In previous publications [5], [6], the fields of RF surface coils without dielectric substrate materials were calculated by the method of moments (MoM) [7] for near field analysis. In this paper, the recently used microstrip transmission line resonator element consisting of a thin conducting strip placed on a dielectric substrate with a metallic conductor ground plane is firstly analyzed with the CFIE in high field MRI systems. In the present method, tetrahedra of with the Schaubert-Wilton-Glisson (SWG) [8] basis functions are used for the transmission line resonator element, and the Rao-Wilton-Glisson (RWG) [9] basis functions with surface triangular patches are used for the surface currents. The technique is demonstrated with a spherical phantom filled with brain-equivalent material. The single transmission line resonator element is modeled for the 9.4 T MRI system (Larmor frequency ~ 400 MHz) and subsequently, the RF magnetic fields in the phantom are calculated for eight channel resonator arrays by superposition and they are compared to the FDTD results. Accurate and efficient results for the internal B_1 field in the phantom are obtained. In addition, an approach finding optimum amplitude and phase excitation parameters for a selected region of interest is discussed.

2. Methodology

In RF resonator analysis at high B_0 static fields, the combined field integral equations are solved by the method of moments and the equivalent surface currents on the phantom are calculated.

For dielectric scatterers, the combined field integral equation (CFIE) formulation may be used to find the equivalent currents on the enclosing surface. In order to transform the combined integral equation into a matrix equation, the surface of the object has a triangular patch model with Rao-Wilton-Glisson (RWG) basis functions. Once unknown current coefficients [J] and [M] are determined, the scattered fields in region 1 and 2 in Fig. 1 are directly evaluated. The transmission line resonator is analyzed without scattering objects. Modified basis functions, Schaubert-Wilton-Glisson (SWG) basis functions [8] are used since a thin metal strip resonator with the dielectric substrate may require a volume integral equation [10]. These SWG basis functions possess artificial volume charges whose effect becomes apparent close to the dielectric-metal interface of the transmission line elements. This modeling method also results in an impedance matrix described in [8], then the scattered electric and magnetic fields are calculated at the resonant frequency of this element. The Green's functions method [11] may be used to analyze a general microstrip geometry but it assumes an infinite ground plane, which is not the case here.

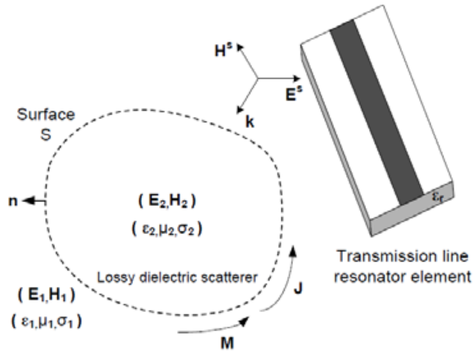

Figure 1: Geometry of a lossy dielectric scatterer with a transmission line resonator element in free space.

3. Results and Discussion

The half-wavelength transmission line resonator element which is a microstrip line, with center feed at 400 MHz for the 9.4 T MRI system was used in these simulations. Subsequent simulations will use a fore-shortened line with shunt capacitors and end fed elements. In Fig. 2, the dimension of the transmission line resonator element is shown and the relative substrate dielectric constant, □r = 2.2 is used. To find the resonant frequency, input impedance and return loss (S11) are plotted in Fig. 2. At approximately 400 MHz, the input resistance is about 45 Ω and the input reactance is nearly zero. For the present case, 838 triangles, 1197 metal edges, 2261 dielectric edges, and 1638 tetrahedra were used. The matrix is solved by Matlab with 27s of CPU time (Intel Core2 Duo CPU 2.53 GHz) at each frequency, with 9s for constructing the impedance matrix. The transmit B_1+ and receive B_1- fields in the axial slice of the center of the phantom with excitation of one element are plotted in Fig. 3(a) and 3(b) and the CFIE results are compared to the FDTD results. At the center point in Fig. 3(a), the difference is approximately 0.0013 (-28 dB). As expected in high magnetic field MRI systems1 and B_1 have typical twisted amplitude profiles with similar shapes but opposite directions. Fig. 4 illustrates the B_1+ field distributions depending on the position of the region of interest and compares the results from the 16 and 32 channel coils. In this simulation, three positions of the region of interest (ROI) are chosen as shown in Fig. 4(a) and the convex optimization with an iterative method was applied to determine the amplitude and phase of the currents driving individual coil elements. When the ROI is located near the edge homogeneity in the outside ROI is poorer, especially for the 16-channel coil excitations (Fig. 4(b)). The 32-channel results are much better when compared to those from the 16-channel coil for all positions of the ROI. The homogeneity coefficient is also reduced by approximately 25-30 % as shown in Fig. 4(d) and 4(e).

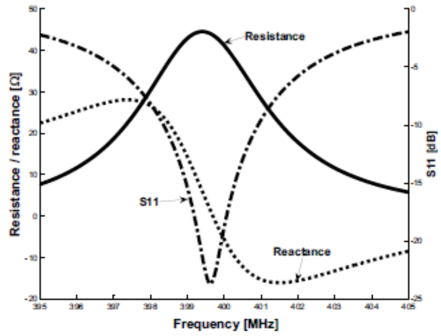

Figure 2: Input impedance and return loss (S11) of the transmission line resonator element.

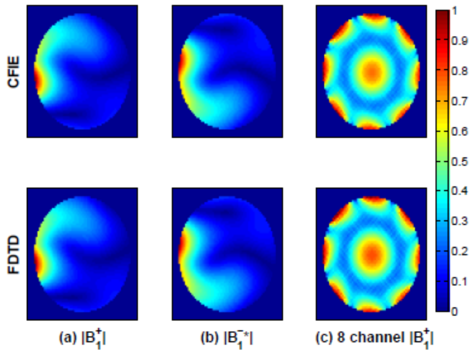

Figure 3: Comparison of B_1 maps on the center of the sphere.
Normalized $B1$ fields in the transaxial slice in the 9.4 T MRI system.

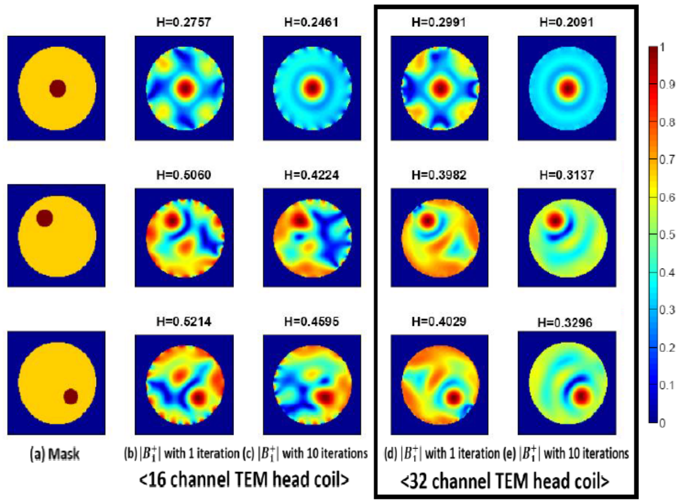

Figure 4: Localization results at 9.4 T (400 MHz) in a phantom model.

5. Conclusion

The combined field integral equation (CFIE) method to analyze the B_1 fields using transmission line resonators in high field MRI systems has been demonstrated. The CFIE method provides good modeling flexibility and solution accuracy for coils and phantoms by using triangular patches and the RWG basis functions. After modeling the resonator microstrip element at the resonant frequency and obtaining the equivalent current unknowns over the phantom, the internal fields in the phantom were calculated. Numerical results show rapid and efficient B_1 fields in the 9.4 T MRI system. In this paper, the result in a single transmission line element with the phantom is presented and the proposed method is to be extended to human models for RF B_1 shimming for multi channel resonators in high field MRI systems with further modifications. A method varying the amplitude and phase of driving individual resonator element is also discussed.

References

[1] J. Vaughan , M. Garwood, C. Collins, W. Liu, L. DelaBarre, G. Adriany, P. Anderson, H. Merkle, R. Goebel, M. Smith, and K. Ugurbil, “7 T vs. 4T : RF power, homogeneity and signal to noise comparison in head images,” *Magnetic Resonance in Medicine*, vol. 46, pp. 24-30, 2001.

[2] J. Vaughan, L. DelaBarre, C. Snyder, J. Tian, C. Akgun, D. Shrivastava, W. Liu, C. Olson, G. Adriany, J. Strupp, P. Anderson, A. Gopinath, and P-F. Moortele, “9.4 T human MRI: Preliminary results,” *Magnetic Resonance in Medicine*, vol. 56, pp. 1274-1282, 2006.

[3] J. Vaughan, C. Snyder, L. DelaBarre, P. Bolan, J. Tian, L. Bolinger, G. Adriany, P. Andersen, J. Strupp, K. Ugurbil, “Whole-body imaging at 7T: Preliminary results,” *Magnetic Resonance in Medicine*, vol. 61, pp. 244-248, 2009.

[4] K. Umashankar, A. Taflove, and S. M. Rao, “Electromagnetic scattering by arbitrary shaped three-dimensional homogeneous lossy dielectric objects,” *IEEE Trans. Antennas and Propagation*, vol. 34, pp. 758-766, 1986.

[5] F. Lin, W. Kuan, S. Jeng, and J. Chen, “Quantitative spectral/spatial analysis of phased array coil in magnetic resonance imaging based on method of moment,” *IEEE Trans. Medical Imaging*, vol. 18, pp. 1129-1137, 1999.

[6] S. Wang and J. H. Duyn, “Analysing radio-frequency coil arrays in high-field magnetic resonance imaging by the combined field integral equation method,” *Physics in Medicine and Biology*, vol. 51, pp. 3211-3229, 2006.

[7] R. F. Harrington, “Field computation by moment mothods,” *IEEE PRESS* (1993).

[8] D. H. Schaubert, D. R. Wilton, and A. W. Glisson, “A tetrahedral modeling method for electromagnetic scattering by arbitrarily shaped inhomogeneous dielectric bodies, ” *IEEE Trans. Antennas and Propagation*, vol. 32, pp. 77-85, 1984.

[9] S. M. Rao, D. R. Wilton, and A. W. Glisson, “Electromagnetic scattering by surfaces of arbitrary shape, ” *IEEE Trans. Antennas and Propagation*, vol. 30, pp. 409-418, 1982.

[10] S. N. Makarov, “Antenna and EM Modeling with MATLAB,” *Wiley*, 2002.

[11] M. Irsadi and R. Mittra, “Derivation of closed-form Green’s functions for a general microstrip geometry, ” *IEEE Trans. Microwave Theory and Techniques*, vol. 40, pp. 2055-2062, 1992.

Acknowledgments

This research was supported by Basic Science Research Program through the National Research Foundation of Korea (NRF) funded by the Ministry of Education, Science and Technology (2011-0014776).